

DETERMINATION OF GRAIN SIZE DISTRIBUTION FROM NMR RELAXATION TIME USING PORE SCALE MODELING

J. Chen, M. Gladkikh, S. Chen, D. Jacobi, and H. Kwak, Baker Hughes, Houston, TX.

*This paper was prepared for presentation at the International Symposium of the
Society of Core Analysts held in Calgary, Canada, 10-12 September, 2007*

ABSTRACT

This paper describes a new approach of using pore scale geometric modelling to determine grain size distribution from NMR relaxation time logging measurements. In particular, it focuses on quartzose and feldspathic sandstones. This approach was tested with various unconsolidated sand samples, Berea outcrops, and reservoir sandstone cores. Results indicate that mineralogy (for example, quartz vs. feldspar) is important in the determination of grain size distribution from T_2 , because grain surfaces change with mineralogy and are affected by weathering, dissolution, and other diagenetic processes. A parameter, called surface roughness factor, is introduced to account for these effects. The two scenarios we studied are (a) quartz-only and (b) quartz plus altered feldspar grains (for example, plagioclase feldspar). For the quartz dominated case, the product of the surface relaxivity and surface roughness factor is $33.7 \pm 6.5 \mu\text{m}/\text{sec}$ for all the tested samples. For the case of quartz plus altered feldspar grain, we observed that the surface roughness factor of the altered feldspar grains linearly increases with its weight percentage. The grain size distribution calculated using this approach agrees well with the measured values. The results of this study removes some uncertainty arising from using NMR relaxation time distribution for estimation of grain size distribution.

INTRODUCTION

Determination of grain size distribution is important to sand management of unconsolidated formations (Oyeneyin et al., 2005), for predicting depositional and diagenetic facies and hydraulic units, and for estimating penetration depth in perforation (Brooks et al., 1998). The traditional methods of measuring grain size distribution include sieve analysis or laser particle size analysis using unconsolidated particles, and image analysis of thin sections for consolidated rocks. Alternatively, NMR T_2 distribution is often recognized to be related to grain size distribution by correlating T_2 with pore size and subsequently correlating pore size with grain size. For example, for some over-simplified systems such as the cubic or rhombohedral packing of uniform spheres (Figure 1), the relationship between S/V and grain size and thus T_2 and grain size is well determined (Eq. 1).

$$\frac{1}{\rho_2 T_2} = \frac{S}{V} = \frac{3(1-\phi)}{\phi \cdot r_g} \quad (1)$$

Where ρ_2 is surface relaxivity, S/V is the ratio of grain surface to pore volume, ϕ is porosity, and r_g is grain radius. In Eq. 1, it is assumed that the system is 100% water saturated and the decay due to bulk relaxation and diffusion is neglected.



Figure.1 Cubic packing (left plot, porosity 0.48) and rhombohedral packing (right plot, porosity 0.26) of uniform spheres.

Correlation between S/V and grain size and thus T_2 and grain size is much more complicated for natural rocks due to the following reasons. Firstly, natural rock has a distribution of different grain sizes with various shapes instead of uniform spheres. Secondly, natural rock may have a complex mineralogy including quartz, K-feldspar, plagioclase, calcite, dolomite, and various clay minerals such as kaolinite, illite, chlorite, and so on. Thirdly, reservoir rocks have undergone various geological processes such as sedimentation, cementation, compaction, diagenesis, and so on. A pore-scale geometric model calculating S/V and T_2 distribution was used in this study to account for a number of these complex factors. It generates a pore network of tetrahedral pores and throats, connecting them from random dense packing of equal spheres using modified Delaunay tessellation. This procedure provides the exact geometry of each tetrahedral pore for the calculation of S/V distribution and T_2 . The details of the pore-scale geometric model can be found in Gladkikh (2005) and Gladkikh and Mendez (2006).

PROCEDURES

The procedure of the determination of grain size distribution is based on the prediction of T_2 in a model rock constructed by pore scale modeling incorporating the geology and mineralogy of the formation. To compute grain size distribution, we calculate T_2 in the model rock with various grain size distributions. The estimated grain size distribution is derived from the best fit between the measured and predicted T_2 .

Studies show that there exist certain patterns for grain size distribution in natural rocks such as log-normal, Weibull, log-hyperbolic, log-skew-Laplace, and so on, due to different depositional and geological environments (Christiansen et al., 1984; Kondolf and Adhikari, 2000; Barndorff-Nielsen et al., 1982; Purkait, 2006; Wyrwoll and Smyth, 1985). In this study, log-normal and Weibull distributions were used for the pre-construction of the initial grain size distribution. As an example, Eq. 2 and 3 show the trimodal incremental $f(X)$ and cumulative $P(X)$ Weibull distribution.

$$f(X) = \sum_{i=1}^3 \alpha_i \frac{\beta_i}{\gamma_i} \left(\frac{X}{\gamma_i}\right)^{\beta_i-1} \exp\left(-\left(\frac{X}{\gamma_i}\right)^{\beta_i}\right)$$

$$X > 0, \alpha_i > 0, \beta_i > 0, \gamma_i > 0, \sum \alpha_i = 1 \quad (2)$$

$$P(X) = \sum_{i=1}^3 \alpha_i \left(1 - \exp\left(-\left(\frac{X}{\gamma_i}\right)^{\beta_i}\right)\right) \quad (3)$$

where β_i is the shape factor, γ_i is the scale factor, α_i is the intensity. X is defined as follows,

$$X = \ln\left(\frac{r_g}{r_{g,0}}\right) \quad (4)$$

where r_g is grain size, $r_{g,0}$ is the minimum grain size chosen in the pre-construction of grain size distribution.

S/V and T_2 relaxation time distributions are calculated from the knowledge of exact geometry of each tetrahedral pore in pore-scale model. For the simple mineralogy of 100% quartz sand, surface relaxation time $T_{2,s}$ of a single pore is calculated as

$$\frac{1}{T_{2,s}} = \rho_2 \left(\frac{S}{V}\right) \quad (5)$$

Similarly, for a more complex scenario where the pore is formed by grains with multiple mineralogy and/or clay minerals, the $T_{2,s}$ relaxation time of such a pore is calculated as

$$\frac{1}{T_{2,s}} = \left(\frac{\sum_j \rho_{2,j} \cdot S_j}{V}\right) \quad (6)$$

where $\rho_{2,j}$ and S_j are the surface relaxivity and surface area for the j^{th} grain forming the pore. Bulk relaxation and echo decay due to diffusion can be simply added to Eq. 5 and 6 when their contributions to the total relaxation are important, as follows,

$$\frac{1}{T_2} = \frac{1}{T_{2,B}} + \frac{1}{T_{2,S}} + \frac{1}{T_{2,D}} \quad (7)$$

The calculated T_2 relaxation time distribution is fitted with the measured T_2 by minimizing the error function (Eq. 8). During this process, the model parameters in the pre-construction of grain size distribution (Eq. 2 and 3) are determined.

$$g(\alpha_j, \beta_j, \gamma_j) = \min\left(\sum_{i=1}^n (f_i^{calc} - f_i^{meas})^2\right) \quad (8)$$

Where f_i^{calc} and f_i^{meas} are the intensity of the i^{th} bin in the calculated and measured T_2 relaxation time distribution, respectively.

RESULTS AND DISCUSSIONS

The properties (porosity, permeability, and XRD mineralogy) of the Berea core samples in this study are listed in Table 1. They can be divided into two groups according to their bulk mineralogy. One group of cores is quartz dominated, while the other group contains a significant amount of feldspar. As shown in Figure 2, the feldspar (in white circles) has been subject to weathering and dissolution that increases their surface areas. Since the pore-scale modeling is a geometric model starting from the random dense packing of equal spheres with smooth surface, a surface roughness factor is introduced to calculate

the true surface area of the rough surface. This true surface area is what the fluid molecules experience/access in a NMR T_2 relaxation process. The definition of surface roughness factor in this study is as follows,

$$R_s = \frac{S_{true}}{S_{geom.}} \quad (9)$$

where S_{true} and $S_{geom.}$ are the true surface area and geometric surface area, respectively.

Table 1 porosity, permeability and mineralogy of the Berea cores used in this study

Core #	B7	B9	B10	B11	B12	B8	B1	B2	B3	
Porosity (%)	19.2	18.0	18.0	18.5	18.5	17.1	29.8	29.2	30.8	
Air-perm (md)	116.3	80.4	108.4	112.2	76.4	42.8	13263	10385	7155	
Mineralogy	Quartz	86	87	88	89	85	78	47	59	45
	Feldspar	5	3	1	3	3	2	29	32	51
	Carbonate	5	5	5	3	5	14	13	5	1
	Clay	5	5	6	5	7	6	9	4	3
	Anhydrite	0	0	0	0	0	0	2	0	0



Figure 2 Thin sections of Berea core B1 (left) and B3 (right).

For the quartz dominated core samples, the only required parameter in the determination of grain size distribution from T_2 is $(\rho_2 * R_s)$ (Eq. 5 and 9). For the test samples in this study, the grain size distribution was measured so that surface relaxivity could be estimated by matching the calculated and measured grain size distribution (by layer grain size analysis after the core is disaggregated by a commercial lab, verified with thin section grain size analysis). As an example, Figure 3 shows the comparison between the calculated and measured T_2 relaxation time distribution (in the left) and grain size distribution (in the right). For this sample, $(\rho_2 * R_s) = 38 \mu\text{m}/\text{sec}$. For all the quartz dominated samples tested in this study, $(\rho_2 * R_s) = (33.7 \pm 6.5) \mu\text{m}/\text{sec}$.

For the core samples with a complex mineralogy of quartz and feldspar, the required parameters in the determination of grain size distribution from T_2 are ρ_2 , R_s , and the mass percentage of quartz. Similar to Figure 3, Figure 4 shows the comparison between the calculated and measured T_2 relaxation time distributions (in the left) and grain size distributions (in the right) for sample B3. In this calculation, ρ_2 values for quartz and feldspar are 10 and 25 $\mu\text{m}/\text{sec}$; while R_s for quartz and feldspar are 4 and 18, respectively. Note that ρ_2 of the feldspar is larger than that of the quartz. The differences are attributed to surface coatings, of smectite, illite or kaolinite, that have formed from

the weathering or dissolution of the feldspar surfaces. Moreover, R_s of the feldspar is much larger than that of the quartz reflecting the weathering and dissolution process.

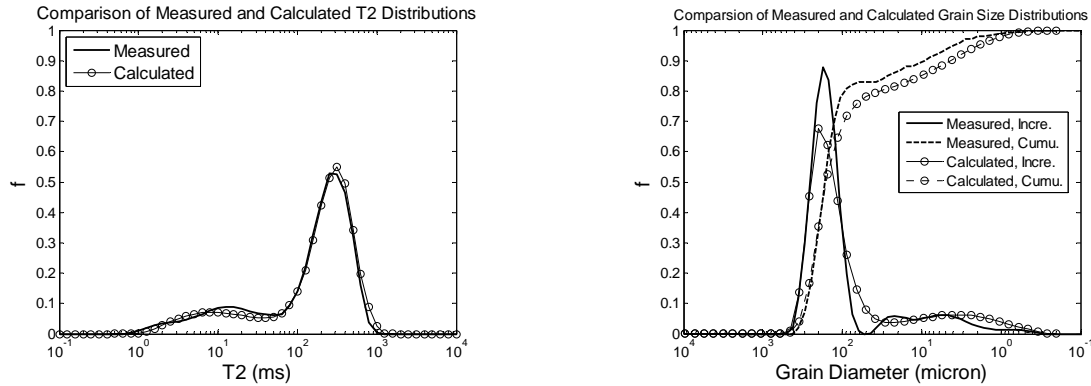


Figure 3 Measured and calculated T_2 (left) and grain size (right) distributions.

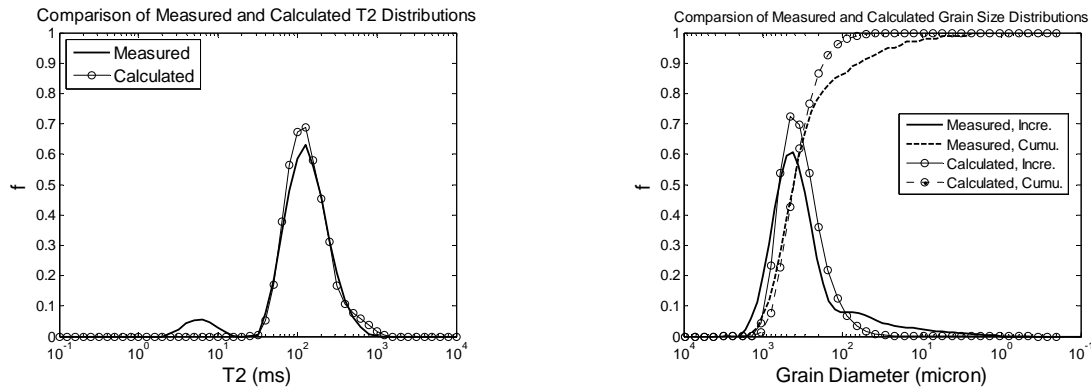


Figure 4 Measured and calculated T_2 (left) and grain size (right) distributions for B3.

The surface roughness factor of the altered feldspar grain for all the cores with complex mineralogy is shown in Figure 5. We observed that surface roughness factor of the altered feldspar grain increases linearly with its weight percentage. Note that the surface roughness factor at the end point of 0% wt has taken into account of the different values of surface relaxivity for quartz (10 $\mu\text{m}/\text{sec}$) and altered feldspar grain (25 $\mu\text{m}/\text{sec}$).

Figure 6 shows the comparison of measured and calculated grain size (mode value) for all the cores studied in this paper.

CONCLUSIONS

This paper developed a new methodology for the determination of grain size distribution from T_2 using pore-scale geometrical modeling. We found out that mineralogy affects the surface to volume ratio S/V through weathering, dissolution and other diagenesis processes. A parameter, called the surface roughness factor R_s was introduced to account for these effects. Moreover, this paper considered two types of sedimentary rocks for the determination of grain size distribution from T_2 . One is quartz dominated case; the other

is the case of quartz plus altered grain (for example, plagioclase feldspar in this paper). For the quartz dominated case, $(\rho_2 * R_S) = 33.7 \pm 6.5 \mu\text{m}/\text{sec}$. For the case of quartz plus altered feldspar, it was observed that R_S increases linearly with its weight percentage. Finally, the calculated grain size distribution using this approach agrees well with the measured value.

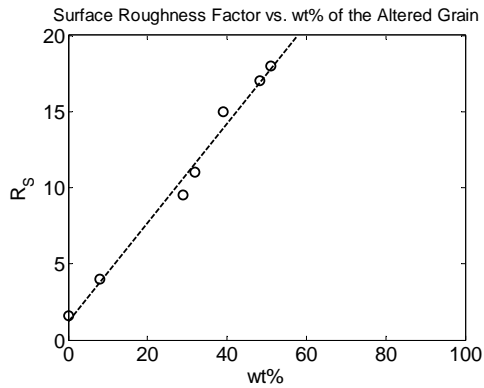


Figure 5 Correlation between R_S of feldspar vs. its weight percentage.

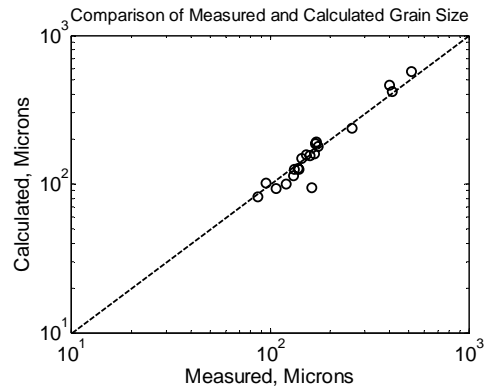


Figure 6 Comparison between measured and calculated grain size (mode value).

REFERENCES

- Barndorff-Nielsen O., Dalsgaard K., Halgreen C., Kuhlman H., and Shou G., "Variations in particle size distribution over a small dune," *Sedimentology*, (1982), **29**, 53-65.
- Brooks J. E., Yang W., and Behrmann L. A., "Effect of sand-grain size on perforator performance," *SPE International symposium on formation damage control*, (1998), SPE 39457.
- Christiansen C., Blaesild F., and Dalsgaard K., "Re-interpreting 'segmented' grain size curves," *Geological Magazine*, (1984), **121**, 47-51.
- Gladkikh M., A priori prediction of macroscopic properties of sedimentary rocks containing two immiscible fluids, *PhD Dissertation Thesis*, (2005), University of Texas at Austin, Austin, TX, USA.
- Gladkikh M., and Mendez F., "A pore-level approach petrophysical interpretation of well logging measurements," *XVI International Conference in Computational Methods in Water Resources*, (2006).
- Kondolf G. M., and Adhikari A., "Weibull vs. lognormal distributions for fluvial gravels," *Journal of Sedimentary Research*, (2000), **70**, 456-460.
- Oyeneyin M. B., Macleod C., Oluyemi G., and Onukwu A., "Intelligent sand management," *29th Annual SPE International Technical Conference and Exhibition*, (2005), SPE 98818.
- Purkait B., "Grain-size distribution patterns of a point bar system in the Usri river, India," *Earth Surface Processes and Landforms*, (2006), **31**, 682-702.
- Wyrwoll K. H., and Smyth G. K., "On using the log hyperbolic distribution to describe the texture characteristics of Eolian sediments," *Journal of Sedimentary petrology*, (1985), **55**, 471-478.